

Short-Term Responses of Apple Fruit to Partial Reoxygenation during Extreme Hypoxic Storage Conditions

Stefano Brizzolara,[†] Dubravka Cukrov,[†] Massimo Mercadini,[‡] Federico Martinelli,[§] Benedetto Ruperti,^{||} and Pietro Tonutti^{*,†}

[†]Life Sciences Institute, Scuola Superiore Sant'Anna, Piazza Martiri della Libertà, 33, 56127 Pisa, Italy

[‡]Marvil Engineering, Zona Produttiva SCHWEMM, 8, 39040 Magrè Sulla Strada del Vino, Bolzano, Italy

[§]Department of Biology, University of Florence, Sesto Fiorentino, Via Madonna del Piano, 6, 50019 Sesto Fiorentino, Firenze, Italy

^{||}Department of Agronomy, Food, Natural Resources, Animals and Environment, University of Padova, Viale dell'Università, 16, 35020 Legnaro, Padova, Italy

S Supporting Information

ABSTRACT: The short-term (24 h) responses of apple fruit (cv. 'Granny Smith') to a shift in the oxygen concentration from 0.4 to 0.8 kPa, a protocol applied in the dynamic controlled atmosphere (DCA) storage technique, have been studied. Metabolomics and transcriptomics analyses of cortex tissue showed an immediate down-regulation of fermentative metabolism and of the GABA shunt in parallel with the activation of several 2-oxoglutarate-dependent dioxygenase genes. Down-regulation of the free phenylpropanoid pathway genes and the diversion of propanoid synthesis toward the methyl-erythritol phosphate route were also observed. Partial reoxygenation induced increases of glyceric, palmitic, and stearic acids and of several phosphatidylcholines and phosphatidylethanolamines and decreases of specific amino acids (valine, methionine, glycine, phenylalanine, and GABA), organic acids (arachidic and citric acids), and secondary metabolites (catechin and epicatechin). The oxygen shift also resulted in transcriptional rewiring of several components of IAA and ABA regulation and signaling. These results provide novel insights on the complexity of the short-term physiological responses of apple fruit to partial reoxygenation applied during DCA storage.

KEYWORDS: *dynamic controlled atmosphere (DCA), postharvest, low oxygen, metabolomics, transcriptomics, Malus domestica*

■ INTRODUCTION

Advancements in our knowledge of apple-fruit postharvest physiology and technical improvements have recently led to the development of protocols based on the dynamic modulation of low-oxygen concentrations during controlled atmosphere (CA) storage.¹ The dynamic controlled atmosphere (DCA) technique is based on the use of oxygen levels that are kept at extremely low values (about 0.3–0.4 kPa), close to the anaerobic compensation point (ACP). These hypoxic conditions, which are considered the lowest oxygen limit (LOL) tolerated by fruit, are in general effective in retaining firmness and acidity together with better scores for crispness and skin color if compared with oxygen concentrations above the LOL.^{2–7} In addition, reduced incidence of cold-storage disorders, such as superficial scald has been reported in DCA-stored apples.⁸ These results, which can vary greatly in relation to the genetic background, can be achieved if the DCA protocol is properly applied through strict control of the physiological responses of apples, which may react negatively if extreme hypoxic-stress conditions (at or slightly above the LOL) are applied for too long. This results in the accumulation of anaerobic metabolites and loss of quality (e.g., off flavors and flesh browning). On the basis of specific parameters that are effective in assessing the stress level reached by the fruit (ethanol production, chlorophyll fluorescence, and respiratory quotient), oxygen is adjusted (increased) to the considered “safe” concentration (about 0.8–

0.9 kPa) that could be maintained until the end of the storage period, or repeated adjustments of oxygen levels can be applied depending on the physiological and technological parameters. Plant tissues, including fruit, are highly sensitive and respond differently to slight changes in oxygen concentration, most likely through modulation of the recently discovered oxygen-sensing mechanism (N-end-rule pathway) involving ethylene-responsive factors (ERFs).^{9,10} Cukrov et al.¹¹ reported that ‘Granny Smith’ apples react differentially in terms of both gene expression and metabolic changes, when postharvest hypoxic conditions are set at 0.4 or 0.8 kPa of oxygen, and this occurs early after hypoxia is imposed. In fact, the accumulation of specific metabolites (e.g., alanine and GABA) and transcripts (e.g., alcohol dehydrogenase, *ADH*; pyruvate decarboxylase, *PDC*; alanine amino transferase, *AlaAT*; and sucrose synthase, *SuSy*) shows significant changes already after 3 days of incubation under the two different conditions. This indicates the presence of mechanisms highly sensitive and quickly reacting to even moderate changes in oxygen levels surrounding the fruit. Reoxygenation after anoxic stress has a profound and rapid impact, as observed in model species. Anaerobically grown rice seedlings resulted in rapid tran-

Received: January 2, 2019

Revised: April 8, 2019

Accepted: April 9, 2019

Published: April 9, 2019

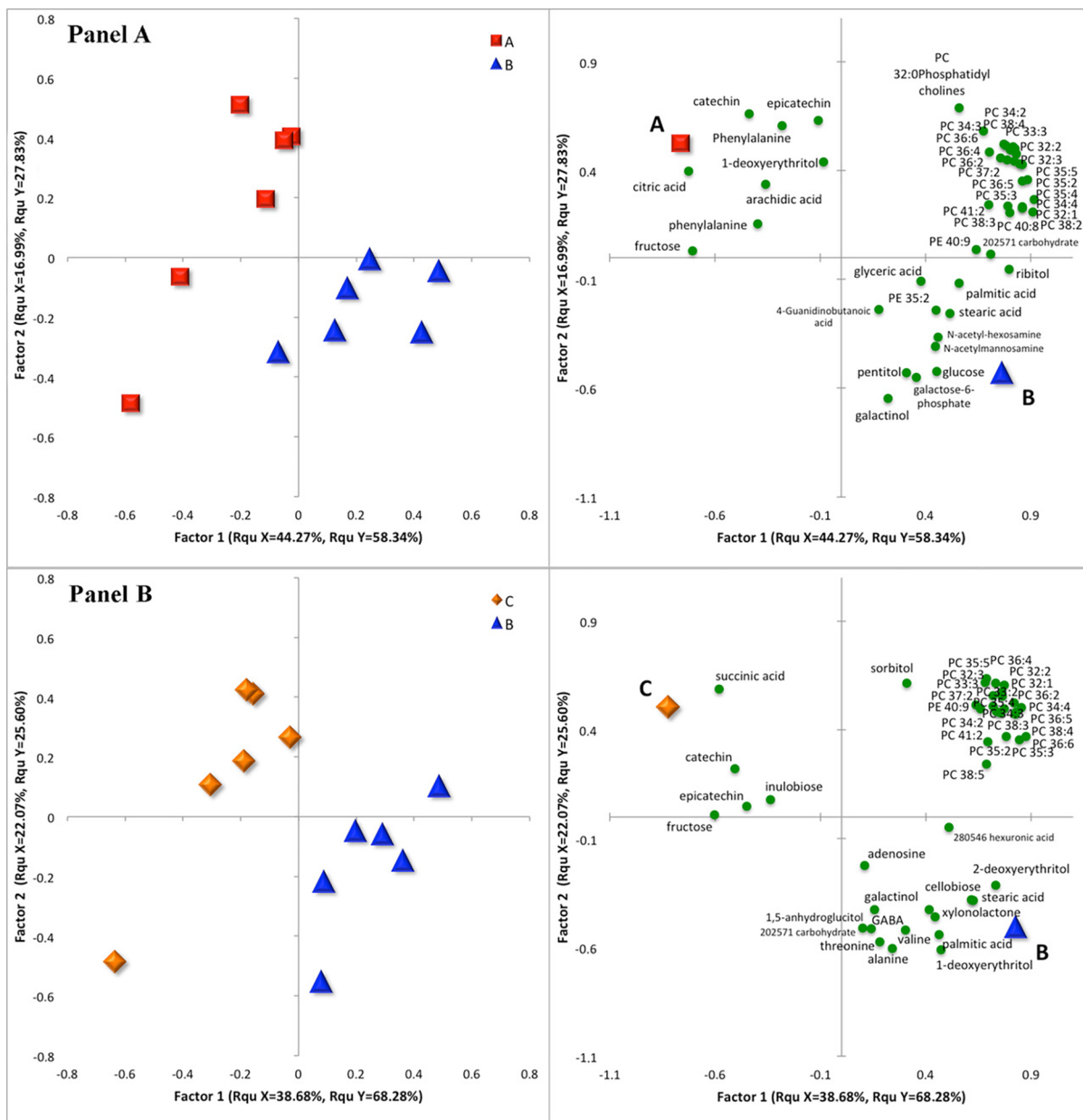


Figure 1. Partial least squares discriminant analysis (PLSDA) performed on the whole set of identified metabolites, comparing (Panel A) sample set A (24 DIA of 0.4 kPa of oxygen) vs B (31 DIA, sampled 24 h after the shift from 0.4 to 0.8 kPa) and (Panel B) sample set B vs C (31 DIA of 0.8 kPa of oxygen). Blue triangles, B samples; red squares, A samples; orange diamonds, C samples. Variable-importance-in-projection (VIP) scores were used to filter important features contributing to the clustering.

scriptomic changes in DNA methylation after reoxygenation,¹² and *Arabidopsis* cell cultures immediately respond to anoxia and subsequent reoxygenation, activating the antioxidant machinery.¹³ Also, fruit tissues appear to quickly react to changes in atmosphere composition. Trobacher et al.¹⁴ reported that removal of the stress conditions applied during static CA, rapidly (3 h) resulted in a net decline in GABA levels in cultivar ‘Empire’ apples. No information is available concerning the short-term metabolic and molecular reactions of fruit tissues to slight changes in oxygen concentration, as those used in DCA protocols, that depending on the cultivar and the storage duration, may apply one or repeated low-oxygen fluctuations. Considering both fruit-physiology and storage-technology issues, the goal of this paper was to evaluate by metabolomic and transcriptomic profiling the responses of

‘Granny Smith’ apples 24 h after the oxygen concentration shifted from 0.4 to 0.8 kPa.

■ MATERIALS AND METHODS

Plant Material and Treatments. Apple (*Malus domestica* Borkh., cv. ‘Granny Smith’) fruit were treated as reported in Cukrov et al.¹¹ Briefly, harvested fruit (starch index of 7, based on a 1 to 10 scale) were selected and immediately stored in three refrigerated (1 °C) experimental chambers under normoxia. After 3 days of acclimation of fruit to low temperature, 0.4 (0.4ox) and 0.8 (0.8ox) kPa oxygen atmospheres (in nitrogen and 0.9–1 kPa of CO₂) were applied in two different chambers. On day 30, when ethanol accumulation reached the threshold value of about 75 mg/L, oxygen concentration was increased from 0.4 to 0.8 kPa. Fruit samples were collected as follows:

(A) After 24 days in atmosphere (DIA) of 0.4 kPa of oxygen

(B) After 31 DIA (30 days at 0.4 kPa of oxygen and 1 day at 0.8 kPa of oxygen, sampled 24 h after the oxygen shift)

(C) After 31 DIA of 0.8 kPa of oxygen

Slices (about 1 cm thick) of cortex tissue (including both inner and outer parts) isolated from the equatorial parts of three fruit collected at different sampling dates were immediately frozen in liquid nitrogen and stored at -80°C .

Metabolic Profiling. Sample analyses were performed at West Coast Metabolomics Center, UC Davis Genome Center. Six replicates (three biological replicates with two technical repetitions each) were analyzed for each treatment. Cortex tissue was ground in liquid nitrogen and lyophilized. Sample extracts were prepared starting from 20 mg of lyophilized material that was added to 1 mL of prechilled extraction solution, and the extraction procedure was performed as described by Fiehn.¹⁵ An aliquot of 20 μL of supernatant was completely dried in a SpeedVac concentrator. Derivatization was performed with methoxyamine and *N*-methyl-*N*-(trimethylsilyl) trifluoroacetamide as described by Fiehn.¹⁵ GC-MS analysis was conducted with an Agilent 6890GC gas chromatograph (GC) coupled to a quadrupole mass spectrometer (MS) and equipped with a 30 m RTx-5Sil column (0.25 μm , 95% dimethyl-5% diphenyl polysiloxane film) with an additional 10 m guard column (Restek). Samples (1 μL) were introduced in both splitless and split modes. The temperature program from 50 to 275 $^{\circ}\text{C}$ at 12 $^{\circ}\text{C}/\text{min}$, with this temperature then held for 3 min. For the splitless conditions, a helium (carrier gas) purge flow of 10.5 mL/min was applied for 1 min (8.2 psi). The split ratio was 1:10, and the split flow rate was 10.3 mL/min. The carrier gas was flowed constantly at 1 mL/min. HILIC-Q-TOF-MS analysis was conducted on an Agilent 1290 UHPLC equipped with a Waters Acuity 1.7 μm BEH HILIC 2.1 \times 150 mm column for separation. An Agilent G6530A accurate-mass QTOF was used with an Agilent ESI Jet Stream ion source. Mobile phases were composed by solvent A (5 mM ammonium acetate with 0.2% acetic acid) and solvent B (9:1 acetonitrile–water with 5 mM ammonium acetate and 0.2% acetic acid). Dry samples were resuspended in 100 μL of solvent B and then column-injected following these conditions: from 0 to 4 min, isocratic 100% B; from 4 to 12 min, B linearly reduced to 45%; and from 12 to 20 min, isocratic 45% B. At the end 20 min, the re-equilibration phase was applied before injection of the samples. The mass spectrometer was a Leco Pegasus IV time-of-flight controlled by Leco Chroma TF software 2.31. The transfer line was held at 280 $^{\circ}\text{C}$, and the ion source was at 250 $^{\circ}\text{C}$. Electron-impact ionization was employed at 70 V with a source temperature of 250 $^{\circ}\text{C}$. The relative concentrations for each metabolite were obtained by peak areas. Identification of metabolites was performed using the Agilent Fiehn GC-MS Metabolomics RTL Library as previously described by Martinelli et al.¹⁶

All data analysis was performed using SAS software (SAS Institute). A normality test was conducted for each metabolite using the Shapiro–Wilk test ($p > 0.01$). Only metabolites that passed the normality test were analyzed using ANOVA ($p < 0.05$), and partial least squares discriminant analysis (PLSDA) was performed as described by Brizzolara et al.⁷

RNA-Seq Analysis. RNA extraction, RNA-seq analyses, data processing, and fold-change (FC) gene expression assessments of the A samples (0.4ox, 24 DIA) versus the B samples (0.4ox, sampled 24 h after the oxygen shift) were performed as described in Cukrov et al.¹¹ GO enrichment and changes in the pathways were analyzed using Plant MetGenMAP analysis package considering identified DEGs (FDR < 0.05).¹⁷

RESULTS

1. Metabolic Profiles. A total of 115 metabolites were identified by applying the two metabolomic approaches. Seventy of them were identified by GC-MS analysis, and 45 were identified by the HILIC method. Nine additional metabolites were partially categorized, 5 as carbohydrates, 3 as trisaccharides, and 1 as hexuronic acid, for a total of 124 metabolites (Table S1, Supporting Information).

The data set containing all the detected metabolites was used to perform targeted multivariate analysis (PLSDA). In the first approach, the three samples were considered together. This analysis showed clear separation of the three samples (Figure S1, Supporting Information). This PLSDA model explains 69.4% of the variability present in the data set. Sample set C (31 DIA of 0.8 kPa of oxygen) appeared strongly related to succinic acid. Galactinol, stearic acid, 2-deoxyerythritol, cellobiose, pentitol, and hexose amino-2-deoxy were significantly higher in sample set B (31 DIA, sampled 24 h after the shift from 0.4 to 0.8 kPa), whereas sample set A (24 DIA of 0.4 kPa of oxygen) showed the highest amino acid levels (valine, methionine, threonine, alanine, serine, phenylalanine, and GABA; Figure S1, Supporting Information).

Additional PLSDA analysis was performed by separately comparing A versus B (Figure 1A), B versus C (Figure 1B), and C versus A (data not shown). In all cases, multivariate analysis revealed high percentages of explained variation, accounting for 95.9% when comparing C versus A, 93.9% for B versus C, and 86.1% for A versus B. These data indicate that in the apple cortex, tissue-specific metabolic changes were already induced 24 h after the oxygen-concentration shift from 0.4 to 0.8 kPa. Moreover, the percentage of variability explained by the models seems to indicate that the differences between sample sets A and B were less extreme than the ones existing between sample sets B and C.

Considering the A versus B comparison (Figure 1A), the two resulting clusters were clearly separated. This contrast points out differences that can be due to the shift in oxygen concentration for the B samples applied 24 h before sampling. In fact, on the basis of the paper of Cukrov et al.,¹¹ the most pronounced changes in specific metabolite contents occurred in the first 2–3 weeks of hypoxic storage: this suggests that the differences observed in this comparison are indeed due to the shift in oxygen concentration and that only negligible effects are due to the different storage durations of the samples (24 vs 31 DIA). Sample set A was more correlated with flavonol compounds, namely, catechin and epicatechin; organic acids, such as arachidonic and citric acid; and other metabolites, such as phenylalanine, fructose, and 1-deoxyerythritol. On the other hand, sample set B was linked to changes in the levels of several sugars and sugar alcohols (such as glucose, 202571_carbohydrate, glucose-6P, galactinol, pentitol, ribitol) but also to *N*-acetylmannosamine; *N*-acetyl-D-hexosamine; and glyceric, palmitic, stearic and 4-guanidinobutanoic acids. Sample set B was also correlated with higher levels of phosphatidylcholines (PCs) and phosphatidylethanolamines (PEs).

When the B samples were compared with the C samples (Figure 1B), the two groups were shown to sit in opposite quadrants, demonstrating pronounced differences. Sample set C (31 DIA of 0.8 kPa of oxygen) appeared to be correlated to succinic acid; fructose; inulobiose; and flavonols, namely, catechin and epicatechin. Sample set B (31 DIA, 30 days at 0.4 kPa of oxygen and sampled 24 h after the shift from 0.4 to 0.8 kPa) appeared instead to be more linked to cellobiose, sugar alcohols (such as galactinol, 1-deoxyerythritol, 2-deoxyerythritol, and 1,5-anhydroglucitol), amino acids (namely, alanine, GABA, threonine, and valine), fatty acids (such as palmitic and stearic acids), and 280546_hexuronic acid. These samples were also characterized by higher levels of adenosine, xylonolactone, PCs, and PEs. Multivariate analyses indicated

Table 1. Metabolites Showing Significant Differences under Variable Low-Oxygen Storage Conditions^a

	succinic acid ^b	2-deoxyerythritol	sorbitol	ribitol	GABA	methionine	valine ^b
<i>p</i> -value	0.0028	0.0001	0.0077	0.0320	0.0344	0.0382	0.0148
sample set A	116.2a	921.2a	187 056a	4149.4a	4010.5a	824.2a	5336.8a
sample set B	144.1a	1256.9b	271 838b	4746.2b	2937.7b	541.6b	875.2ab
sample set C	348.3b	378.1c	262 914b	4836.4b	2412.0b	577.5b	629.3b

^aCompounds were filtered on the basis of their conformity with ANOVA assumptions; 2-deoxyerythritol, sorbitol, ribitol, GABA, methionine, and hexoseamino-2-deoxy fulfilled these requirements and were significantly different among the conditions according to one-way ANOVA tests ($p \leq 0.05$). For each condition, the mean is reported, and letters represent the results of the LSD post hoc test or Dunn test performed after ANOVA or Kruskal–Wallis analysis. ^bSuccinic acid and valine did not meet the ANOVA assumptions but were significantly different among the three groups according to non-parametric Kruskal–Wallis tests ($p \leq 0.05$).

Table 2. Fold Change (FC) between Sample Sets (B vs A and B vs C) in Terms of the Contents of Selected Metabolites^a

compound	FC B vs A	<i>p</i> -value	FC B vs C	<i>p</i> -value	compound	FC B vs A	<i>p</i> -value	FC B vs C	<i>p</i> -value
Section I (B > A, B = C) ^b					Section III (B = A, B > C) ^e				
pentitol	0.18	0.00	0.05	0.26	PC362	0.28	0.14	0.21	0.04
ribitol	0.19	0.01	−0.03	0.41	PC372	0.45	0.06	0.16	0.03
sorbitol	0.54	0.04	0.05	0.43	PC412	0.43	0.07	0.39	0.04
carbohydrate 202571	0.16	0.00	0.08	0.10	Section IV (B = A, B < C) ^f				
carbohydrate 202573	0.21	0.04	0.13	0.07	succinic acid ^d	0.18	0.38	−1.34	0.02
glycerol-3-galactoside	0.21	0.03	0.20	0.11	Section V (B > A, B > C) ^g				
galactose-6-phosphate	0.35	0.03	0.17	0.18	deoxyerythritol 2	0.45	0.00	1.73	0.00
guanidine-butanolic acid 4	0.96	0.01	0.23	0.29	galactinol	0.36	0.04	0.44	0.01
<i>N</i> -acetyl- <i>D</i> -hexosamine	0.74	0.05	0.25	0.24	PC352	0.38	0.05	0.23	0.04
linoleic acid	0.29	0.04	0.06	0.41	PC353	0.35	0.04	0.29	0.02
PC321	0.50	0.01	0.18	0.14	Section VI (B < A, B < C) ^h				
PC344	0.34	0.02	0.20	0.11	citric acid	−0.59	0.00	−0.41	0.00
PC354	0.36	0.01	0.16	0.08	catechin	−0.64	0.01	−0.58	0.01
PC383	0.59	0.01	0.22	0.06	epicatechin	−0.45	0.03	−0.47	0.00
PE343	0.45	0.02	0.23	0.19	^a Compounds were filtered on the basis of their conformity with <i>t</i> -test assumptions; the compounds presented here were significantly different when the groups were compared with <i>t</i> -tests ($p \leq 0.05$). For each molecule, the <i>p</i> -values and the fold changes between conditions are reported. The fold change was calculated with the following formula: FC = log ₂ (average B/average A or C). ^b Compounds in section I showed significant increases in B compared with in A and no differences for B vs C (B > A, B = C). ^c Compounds in section II showed significant decreases in B compared with in A and no differences for B vs C (B < A, B = C). ^d Succinic acid and valine did not meet the <i>t</i> -test assumptions but were significantly different between the test groups according to a non-parametric Kruskal–Wallis test ($p \leq 0.05$). ^e Compounds in section III showed no significant differences for B vs A and significant increases in B compared with in C (B = A, B > C). ^f Compounds in section IV showed no significant differences for B vs A and significant decreases in B compared with in C (B = A, B < C). ^g Compounds in section V showed significant increases in B compared with in A and significant increases in B compared with in C (B > A, B > C). ^h Compounds in section VI showed significant decreases in B compared with in A and significant decreases in B compared with in C (B < A, B < C).				
PE352	0.95	0.03	0.08	0.43					
PE364	0.52	0.04	0.35	0.17					
PE409	0.80	0.03	0.17	0.31					
Section II (B < A, B = C) ^c									
myoinositol	−0.20	0.02	−0.15	0.16					
GABA	−0.45	0.04	0.28	0.12					
glycine	−0.54	0.05	−0.07	0.44					
phenylalanine	−2.27	0.04	−1.07	0.25					
valine ^d	−1.79	0.02	0.50	0.12					
methionine	−0.61	0.04	−0.09	0.36					
Section III (B = A, B > C) ^e									
anhydroglucitol 15	−0.20	0.09	0.59	0.03					
deoxyerythritol 1	−0.15	0.16	0.51	0.02					
cellobiose	0.08	0.34	0.66	0.02					
adenosine	0.31	0.08	0.49	0.02					
alanine	−0.02	0.46	0.59	0.01					
hexuronic acid	0.15	0.06	0.16	0.00					
palmitic acid	0.17	0.06	0.18	0.02					
stearic acid	0.12	0.17	0.27	0.00					

that high variation values characterized B samples compared with A and C samples.

To describe and identify the processes and metabolites that contribute to the discrimination of the samples and are affected by the oxygen shift, ANOVA was applied to analyze metabolites that passed the normality test (Table 1).

Three amino acids differed significantly in their concentrations when the three groups of samples were compared. Two of them (GABA and methionine) showed a significant decrease in the B samples (oxygen shift) when compared with the levels in sample set A (kept for 24 days under 0.4 kPa of

oxygen), but the levels were not statistically different from those detected in sample set C (kept for 31 days at 0.8 kPa of oxygen). A similar trend was observed for valine. In contrast, sorbitol and ribitol showed increases in the samples undergoing the oxygen shift from 0.4 to 0.8 kPa (sample set B), reaching values comparable to those detected in samples constantly kept at 0.8 kPa of oxygen (sample set C). Interestingly, succinic acid showed the highest values in sample C, with sample sets A and B not being statistically different (Table 1). 2-Deoxyerythritol showed higher values in the A and B samples compared with in sample set C.

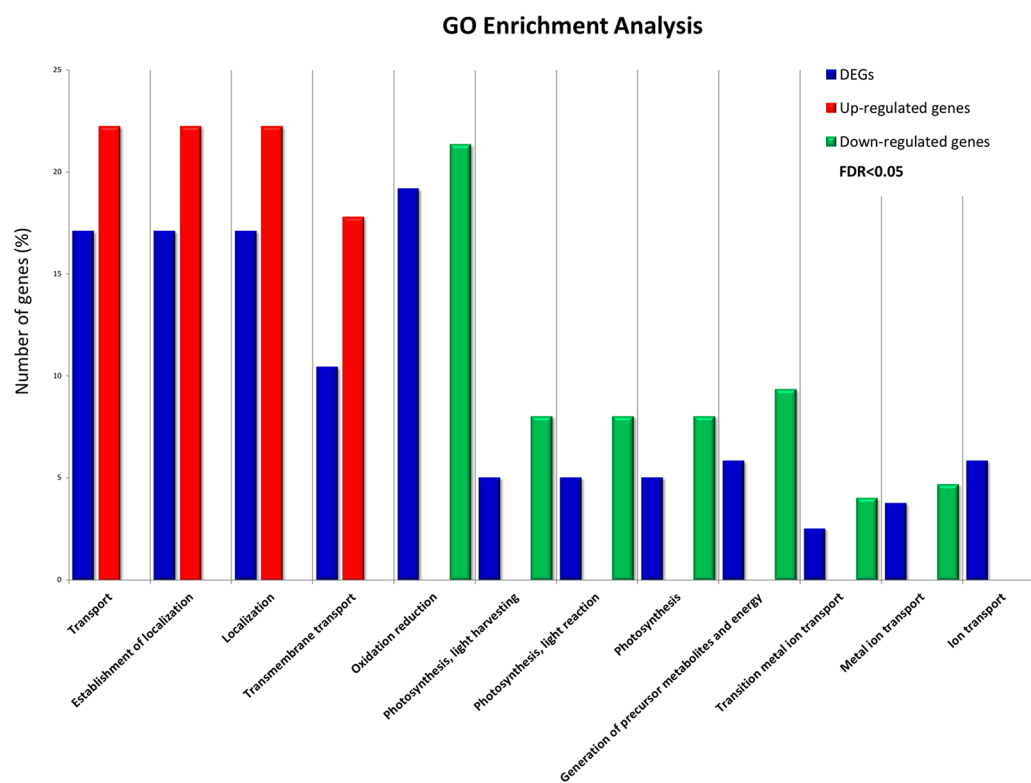


Figure 2. GO-enrichment analysis of the identified DEGs in response to short-term reoxygenation after prolonged hypoxia in apple-cortex cells. Blue histograms report the GO-enriched BPs for all DE genes; red and green histograms report the percentages of the up- and down-regulated DE genes, respectively, in the specific BP categories (FDR < 0.05).

When fold-change analysis was performed to investigate in detail the trend of each specific compound (on the basis of the compound conformity with *t*-test assumptions), flanked by the application of a *t*-test statistical tool, the majority of the identified metabolites showed significant differences between sample sets A and B (Table 2), whereas most of the differences between sample sets B and C were not statistically different (Table 2, sections I and II), indicating that a rapid metabolic reset occurred. Among compounds that showed an increase within 24 h after the oxygen shift, sugar alcohols (pentitol, ribitol, sorbitol, deoxyerythritol, and galactinol) and several PCs and PEs were detected, most of them reaching values not significantly different from those detected in sample set C (Table 2, sections I and V). Other compounds that increased after the oxygen shift were carbohydrates, products of galactose metabolism, and linoleic acid. On the other hand, other fatty acids, namely, the saturated palmitic and stearic acids, did not show significant changes after the oxygen shift, remaining higher than in sample set C (kept at 0.8 kPa; Table 2, section III).

Additional compounds showed a significant decrease 24 h after the shift in oxygen concentration reaching the levels of sample set C (Table 2, section II). Out of the six compounds belonging to this group, five were amino acids. The GABA, glycine, methionine, valine, and phenylalanine contents showed decreases after the oxygen shift, with phenylalanine showing the highest FC value (2.27) between the B and A samples of all identified compounds. Catechin and epicatechin together with citric acid decreased in B compared with in A (Table 2, section VI).

2. Transcript Analysis. In order to identify the main molecular factors involved in apple-fruit-tissue adaptation to

small fluctuations in oxygen availability, the changes of the global transcriptomic (RNA-seq) profiles of sample set B were compared with those obtained from sample set A. A comparison of RNA-seq profiles showed that the subtle increase in oxygen level for apples maintained in hypoxia for about 4 weeks was readily perceived and translated into transcriptomic reprogramming by cortex cells. This in fact resulted in the differential transcriptional expression of 625 genes (DEGs), adopting $|\log FCI| \geq 0.6$ and $|\log qv| < 0.05$ (Table S2, Supporting Information). The quantitative validation of RNA-seq is reported in Table S3 (Supporting Information). Among these DEGs, several *ADH* and phosphofructokinase (*PFK*) encoding genes, as well as one pyruvate-kinase-encoding gene, appeared to undergo down-regulation of transcript abundance following oxygen resupply, confirming the qPCR expression data reported by Cukrov et al.¹¹ and suggesting that the shift from 0.4 to 0.8 kPa of oxygen was already sufficient to trigger a prompt down-regulation of the genes involved in the glycolytic and fermentative pathways (Tables S2 and S4, Supporting Information).

In order to identify enriched gene-ontology (GO) terms in the biological-process (BP) category as a consequence of the short-term oxygen resupply, a GO analysis was performed. Processes that were selectively up-regulated by the reoxygenation included transmembrane transport and transport and establishment of localization and localization, whereas enriched GO terms for down-regulated genes included oxidation–reduction, photosynthesis (light harvesting and light reaction), energy, and transition-metal-ion transport and ion transport (Figure 2).

The regulation of transmembrane-transport-protein-encoding genes, including those of several low-affinity nitrate and

Table 3. Pathways and Genes Identified by Plant MetGenMAP Analysis of the Genes Showing Significant Expression Changes^a between Sample Sets B and A^b

gene ID	closest <i>Arabidopsis</i> homologue, protein family, putative function	pathways	FC B vs A
Section A: Up-regulated Genes			
MDP0000226135	AT3G08040.1, MATE-efflux family protein	Fe(III) reduction and Fe(II) transport	1.86
MDP0000203109	AT1G51340.2, MATE-efflux family protein		2.07
MDP0000903805		amygdalin and prunasin degradation	2.3
MDP0000137211			1.09
MDP0000221213		leucodelphinidin biosynthesis	1.1
Section B: Down-regulated Genes			
MDP0000188700	AT5G54160.1, ATOMT1, OMT1,	methylquercetin biosynthesis, suberin biosynthesis, simple coumarins biosynthesis, free phenylpropanoid acid biosynthesis	-1.00
MDP0000178570	O-methyltransferase 1		-1.16
MDP0000165031			-1.16
MDP0000416307			-1.10
MDP0000208322			-0.95
MDP0000656929			-0.99
MDP0000271872	AT3G02570.1, mannose-6-phosphate isomerase, type I	mannitol biosynthesis	-1.23
MDP0000408705	AT2G21250.1, NAD(P)-linked oxidoreductase superfamily protein		-1.04
MDP0000361351			-1.05
MDP0000818877			-1.03
MDP0000639894			-1.03
MDP0000370937	AT5G66170.3, STR18, sulfur transferase 18	thiosulfate disproportionation III (<i>Rhodanese</i>)	-1.60
MDP0000372061			-1.60
MDP0000272795			-1.50
MDP0000949486		serine biosynthesis, alanine biosynthesis III	-1.06
MDP0000911918			-1.80
MDP0000168387			-1.70
MDP0000300969			-1.77

^aReported as log₂ fold change (FC). ^bSection A, up-regulated pathways and genes. Section B, down-regulated pathways and genes.

sulfate transporters, together with the up-regulation of two nitrate-reductase-encoding genes (Table S2, Supporting Information), is indicative of a concomitant reappraisal of nitrogen and sulfur assimilation as an immediate response to changes in oxygen concentrations. A shift in primary metabolism and amino acid biosynthesis was also identified by pathway analysis, showing the down-regulation of genes encoding enzymes of the mannitol-, serine-, alanine-, and glycine-biosynthesis pathways (Table 3).

The analysis also identified four significantly up-regulated pathways upon oxygen resupply, including Fe³⁺ reduction and Fe²⁺ transport, amygdalin and prunasin degradation, and leucodelphinidin biosynthesis, suggesting prompt regulation of secondary metabolism (Table 3). The rearrangement of secondary metabolism taking place in apple-cortex cells immediately after the oxygen increase was further confirmed by the significant coordinated down-regulation of the pathways responsible for methylquercetin, suberin, simple coumarins, and free phenylpropanoid acid biosynthesis (Table 3). In addition, the concomitant down-regulation of three genes encoding hydroxy methylglutaryl CoA reductase 1 (HMGR1), the rate-limiting step in mevalonic acid biosynthesis, together with the up-regulation of a deoxyxylulose-5-phosphate-synthase-encoding gene, suggested a shift in the isoprenoid-lipid biosynthetic pathway toward the mevalonate-independent and methyl erythrythol dependent route (Table S2, Supporting Information).

Among the DEGs that were most significantly up-regulated in response to oxygen resupply, several genes encoding 2-oxoglutarate-dependent dioxygenases (2-OGDD) were identified, six of them showing an overall doubling of transcript

levels, whereas only three 2-OGDD genes, with lower transcripts counts, appeared to be slightly down-regulated (Table 4).

Several genes involved in iron and heavy-metal homeostasis were simultaneously regulated, eight of which (encoding ferritin, zinc, and heavy-metal transporters) appeared to be among the most down-regulated ones, whereas one (encoding a ferrochelatase) was up-regulated (Table 4).

As far as metabolic signaling and hormone components are concerned, two phospholipase D encoding genes were significantly up-regulated, whereas two genes encoding phospholipases C and D were down-regulated (Table 5), indicating a specific rearrangement of phospholipid metabolism and of phospholipid-dependent signaling. A general rearrangement of hormone responses also appeared to take place as an early oxygen response; this was evidenced by the up-regulation of some genes involved in ABA biosynthesis (9-*cis*-epoxycarotenoid dioxygenases) and in the up-regulation (protein phosphatase 2C) or down-regulation (PYR1-like 4 and GCR2-like 2) of components involved in the ABA-perception–signaling cascade (Table 5). IAA metabolism also appeared to be rapidly impacted by increased oxygen concentrations, with either up- or down-regulation of several components involved in transcriptional control (AUX–IAA transcriptional regulators), IAA conjugation (SAUR-like-, GH3-, indole-3-acetate-, and β -D-glucosyltransferase-encoding genes) and transport (AUX1 and a putative auxin-influx carrier). A few ethylene-responsive signaling elements appeared to be affected through the up-regulation of an ERF2-like gene and the down-regulation of three RAP2.3-

Table 4. Genes Encoding Putative 2-OGDD (Section A) and Proteins Involved in the Regulation of Iron Redox State and Homeostasis (Section B) Identified by RNA-Seq As Showing Significant Expression Changes^a in Apple Cortex between Sample Sets B and A

gene ID	closest <i>Arabidopsis</i> homologue, protein family, putative function	FC B vs A
Section A: 2-Oxoglutarate (2OG) and Fe(II)-Dependent Oxygenase Superfamily Proteins		
MDP0000264351	AT4G10490.1, DLO2, DMR6-like	1.18
MDP0000523205	oxygenase 2, suppressor of downy-mildew resistance, salicylic acid 5-hydroxylase, fine-tuning salicylic acid homeostasis	1.13
MDP0000218810	AT1G52800.1, function unknown	1.01
MDP0000899351	AT1G52800.1, function unknown	1.08
MDP0000175691		
MDP0000843913	AT2G36690.1, putative gibberellin β -hydroxylase-GA biosynthesis (FEII- AO)	0.92
MDP0000523579		0.70
MDP0000181414	AT3G14160.1, function unknown	-0.97
MDP0000142765	AT3G19000.1, function unknown	-1.22
MDP0000156478	AT5G05600.1, JAO2, jasmonate-induced oxygenase 2, jasmonic acid oxidase 2, JOX2	-1.82
Section B: Iron Redox State and Homeostasis		
MDP0000119928	AT5G01600.1, ATFER1, FER1, ferritin 1, regulation of iron and ROS homeostasis	-1.50
MDP0000286750		-1.50
MDP0000189389		-1.65
MDP0000317816		-2.10
MDP0000262639	AT3G11050.1, ATFER2, FER2, ferritin 2, function unknown	-0.83
MDP0000273257	AT3G12750.1, ZIP1, zinc-transporter-1 precursor	-2.09
MDP0000590974		-2.28

^aReported as log₂ fold change (FC).

encoding genes belonging to the hypoxia-inducible ethylene-responsive-element (ERF)-binding protein family¹¹ (Table 5).

DISCUSSION

In order to exploit the beneficial effects of extreme hypoxic conditions, in DCA protocols apples are kept at much lower oxygen concentrations (around 0.4–0.5 kPa) than the levels considered “safe” (around 0.8–0.9 kPa, depending on the genetic background). This concentration is promptly adjusted when fruit metabolic responses (evaluated by means of ethanol production, chlorophyll fluorescence, or RQ) indicate that stress conditions are advanced with high risks of negative physiological reactions and decreases of quality parameters if the same stress conditions are maintained. From a physiological point of view, it is of interest to identify what processes are affected by such a subtle change of oxygen concentration in fruit tissue in the short amount of time.

Our data clearly report that within 24 h from the oxygen shift, a molecular and metabolic rearrangement occurs, with changes in both primary and secondary metabolism. The differential expression of several hundred genes, including those recognized as highly affected by hypoxia (e.g., *ADH*) suggests that the oxygen-sensing mechanisms^{9,10} also present in cortex tissue¹¹ are fine-tuned and perceive subtle changes in oxygen concentration. Indeed, specific ERF-family members have been identified as DEGs (Table 5).

The expression changes detected for genes such as *ADH* and *PFK* clearly indicate that even very subtle changes in oxygen concentrations close to the compensation point are highly effective in inducing rapid readjustments of the glycolytic and fermentative pathways, as already pointed out by Cukrov et al.¹¹ Considering amino acid metabolism, it is recognized that

Table 5. Genes Related to Hormone Perception or Signaling^a and Genes for Phospholipases^b Identified by RNA-Seq As Showing Significant Expression Changes^c in Apple Cortex between Sample Sets B and A

gene ID	closest <i>Arabidopsis</i> homologue, protein family, putative function	FC B vs A
Section A: ABA Biosynthesis and Signal Transduction		
MDP0000437033	AT4G26080.1, ABI1, AtABI1, protein phosphatase 2C family protein	2.78
MDP0000047696	AT2G29380.1, HAI3, highly ABA-induced PP2C gene 3	1.45
MDP0000304124	AT3G51370.1, protein phosphatase 2C family protein	-0.68
MDP0000769041	AT4G19170.1, CCD4, NCED4, 9- <i>cis</i> -epoxycarotenoid dioxygenase 4	1.62
MDP0000744887		1.31
MDP0000145911	AT2G20770.1, GCL2, GCR2-like 2	1.38
MDP0000161117		1.38
MDP0000866489		1.36
MDP0000179084	AT1G72770.1, HAB1, homology to ABI1	0.71
MDP0000134325	AT2G38310.1, PYL4, RCAR10, PYR1-like 4	-0.80
MDP0000270731		-1.40
Section B: Auxin Metabolism, Transport, and Signal Transduction		
MDP0000733506	AT4G15550.1, IAGLU, indole-3-acetate β -D-glucosyltransferase	1.54
MDP0000545122		1.40
MDP0000284467	AT2G14960.1, GH3.1, auxin-responsive GH3 family protein	1.25
MDP0000284467	AT2G33310.2, IAA13, auxin-induced protein 13	0.98
MDP0000250876	AT4G28640.3, IAA11, indole-3-acetic acid inducible 11	0.80
MDP0000295589	AT1G04240.1, IAA3, SHY2, AUX-IAA transcriptional regulator family protein	0.73
MDP000022349	AT1G04250.1, AXR3, IAA17, AUX-IAA transcriptional regulator family protein	-0.93
MDP0000270789	AT2G33310.1, IAA13, auxin-induced protein 13	-1.27
MDP0000277631	AT5G10990.1, SAUR-like auxin-responsive protein family	-1.29
MDP0000312433	AT1G72430.1, SAUR-like auxin-responsive protein family	-1.29
MDP0000596615		-2.37
MDP0000155113	AT2G38120.1, AUX1, MAP1, PIR1, WAV5, transmembrane amino acid transporter family protein	-0.85
Section C: Ethylene Synthesis and Signal Transduction		
MDP0000689946	AT5G47220.1, ATERF-2, ATERF2, ERF2, ethylene-responsive-element-binding factor 2	1.65
MDP0000848905	AT3G16770.1, ATEBP, EBP, ERF72, RAP2.3, ethylene-responsive-element-binding protein	-1.02
MDP0000679280		-1.02
MDP0000566690		-1.02
Section D: Phospholipases		
MDP0000664773	AT2G26560.1, PLAIIA, PLA2A, PLP2, phospholipase A 2A	1.89
MDP0000266144		1.84
MDP0000239522	AT3G08510.1, ATPLC2, PLC2, phospholipase C 2	-0.67
MDP0000125742	AT4G35790.2, ATPLDDELTA, PLDDELTA, phospholipase D delta	-0.70

^aSection A, B, and C. ^bSection D. ^cReported as log₂ fold change (FC).

it may contribute in several ways to mitigate damaging consequences of oxygen limitation.¹⁸ This is the case of GABA, which is recognized as having high physiological activity in stress. GABA levels increase in plant tissues that undergo stresses of different natures, such as hypoxia, and GABA is metabolized via a short pathway known as the GABA shunt.^{19,20} The rapid changes in GABA occurring within 24 h after the oxygen shift (Table 1), when changes in

fermentative pathways and glycolysis also occur, point out that in apple-fruit tissue, GABA may also serve as a signal strictly related to energy balance.²¹ The hypoxia-related GABA increase is the result of the activation of glutamate-decarboxylase (GAD) enzymatic activity and the down-regulation of GABA transaminase (GABA-T), which are responsible for the synthesis and catabolism of GABA, respectively. Trobacher et al.¹⁴ reported that two apple GABA-T genes were likely responsible for the catabolism of accumulated GABA 3 h after the movement of stored apples from controlled to normal atmosphere conditions. The marked decrease of GABA in the partially reoxygenated samples may indicate that recovery of catabolism of this amino acid also rapidly occurs when slight changes of oxygen concentrations are applied.

The up-regulation of several 2-oxoglutarate (2OG) and Fe(II)-dependent oxygenases together with several genes involved in iron homeostasis (Table 4) might indicate a diversion of primary metabolism toward a reactivation of the TCA cycle. 2-OGDDs constitute a large family of highly conserved nonheme Fe²⁺-2-oxoglutarate-dependent dioxygenases that are involved in coupling oxygen sensing and primary metabolism, controlling DNA demethylation and histone proline hydroxylation in animal cells,²² and the synthesis of secondary metabolites such as flavonoids²³ and hormones²⁴ in plants. 2-OGDDs produce succinic acid from oxoglutarate, leading to the hydroxylation of the target molecule. The same enzymes are also responsible for the diversion of oxoglutarate away from the GABA shunt.²⁵ Thus, the regulation of such genes may represent a pivotal hub for coupling sensing of even subtle changes of oxygen with the shift in metabolism in apple-cortex cells. It is noteworthy that the pathway of iron reduction and transport appeared up-regulated, and several genes encoding ferritins (responsible for iron sequestration) were down-regulated following reoxygenation (Figure 2 and Tables 3 and 4). Ferretin, an iron-chelating protein, is also involved in the removal of iron to regulate iron homeostasis in relation to ROS production. Together with the up-regulation of the aforementioned iron-reduction and -transport pathway, these results indicate that regulation of iron reduction (from Fe³⁺ to Fe²⁺) and decreased sequestration for maintaining iron homeostasis are two of the earliest responses to oxygen availability, in order to either maintain ROS control or support 2-OGDD activity, which requires Fe²⁺ and oxoglutarate as obligatory substrates.²²

The shift in secondary metabolism in response to the increase in oxygen levels was evidenced by the down-regulation of catechin and epicatechin levels in the B samples with respect to the A samples. It has been reported that changes in cellular redox homeostasis modulate flavonoid biosynthesis, and in turn, antioxidant flavonoids might act as components of a regulatory circuit of the auxin-signaling pathway.²⁶ Indeed, the highest number of hormone-related genes that appeared to be modulated by the oxygen shift were connected to IAA transport, conjugation, and transcriptional regulation, in addition to ABA biosynthesis and signal transduction, indicating that the regulation of hormonal responses may be a pivotal aspect in low-oxygen adaptation. Considering the phenylpropanoid pathways, genes involved in methylquercetin biosynthesis, suberin biosynthesis, simple coumarins biosynthesis, and free phenylpropanoid acid biosynthesis were down-regulated in the partially reoxygenated samples.

In hypoxic roots, the synthesis of metabolites such as suberin is generally interpreted as a system to prevent oxygen diffusion away from the root tissues through the impermeabilization of the cell walls.²⁷ This response may also be, in part, conserved in fruit. Furthermore, the down-regulation of the suberin-phenylpropanoid pathway in the reoxygenated apple-cortex cells (Table 3) indicates a fast reset of secondary metabolism in response to oxygen, which may be linked to that occurring in the primary and fermentative ones and, possibly, to the up-regulation of 2-OGDD genes. This redirection of secondary metabolism was further evidenced by the down-regulation of three genes encoding hydroxy methylglutaryl CoA reductase 1 (HMGRI), leading to the shutting down of mevalonic acid biosynthesis residing exclusively in the cytosol and ER. The simultaneous up-regulation of a deoxyxylulose-5-phosphate-synthase gene suggests a subcellular shift in the isoprenoid-lipid biosynthetic pathway toward the methyl erythrythol dependent route located in the plastids.

Interestingly, the higher levels of PCs and PEs and lower levels of arachidonic acid, a product of PC and PE metabolism, in samples subjected to reoxygenation (B) in comparison with in the hypoxic samples (A) and in the samples stably kept in 0.8 kPa of oxygen (C, Figure 1 and Table 2) indicate that a transient burst of phospholipid metabolism may be an important part of the early responses and in the generation of regulatory signals in apple-cortex cells facing oxygen resupply. Phosphoglycerides represent a predominant constituent of membranes, and mitochondrial membranes are particularly rich in PCs and PEs.²⁸ Under stress conditions, plant tissues react by altering lipid metabolism. Xie et al.²⁹ reported that in *Arabidopsis* rosettes, the hypoxia-induced lipid changes include significant increases in unsaturated glycerolipid species, phosphatidic acid, and oxidized membrane lipids and decreases in the levels of phosphatidylglycerols (PGs), PCs, and PEs. The selective up-regulation of two genes encoding phospholipase A 2A and the down-regulation of two genes encoding phospholipase C 2 and D delta as well as the observed increases in PCs and PEs in the B samples (24 h after the oxygen shift) indicate that the metabolism of these phospholipids in apples is highly reactive to slight changes in oxygen concentration.

As reported in Figure 2, the GO terms photosynthesis, photosynthetic light harvesting, and light reactions were over-represented. These data indicate that photosynthetic genes are extremely reactive to low-oxygen conditions close to the compensation point, even in tissues and organs where photosynthesis is not active, confirming that higher expression is induced under extreme hypoxic conditions.¹¹

Overall, these data indicate that the short-term reactions of apples to changes in oxygen concentration, such as those applied in DCA protocols, are characterized by selective reconfiguration of C and N metabolism, with the latter showing a general reduction of specific amino acids that accumulate in 'Granny Smith' apples that reached the hypoxic-stress-condition threshold (high levels of ethanol). Interestingly, alanine does not show any significant change 24 h after the oxygen shift. Alanine is known to accumulate in various plant species under hypoxia-anoxia conditions.²⁵ Also, in apple cortex, alanine shows a fast accumulation under low-oxygen storage.^{7,11} In *Arabidopsis* plantlets submitted for 2 h to an anoxic atmosphere, alanine aminotransferase (*AlaAT*) was the only nitrogen-metabolism gene among the core hypoxia-responsive genes to be induced.³⁰ The different trend of

phenylalanine, GABA, glycine, valine, and methionine (decreasing) compared with that of alanine (unchanged) in B samples compared with in A sample indicates the presence of fine-tuned N-metabolism mechanisms during hypoxic stress in apple cortex, with specific pathways quickly responding to even limited changes in oxygen concentration.

In conclusion, investigation of the metabolomic and transcriptomic events occurring in apple-cortex cells within 24 h after partial reoxygenation following a period of long exposure to extreme hypoxia has identified four major events as the earliest clear regulatory responses to new oxygen supply, which included four major areas of physiological–metabolic rearrangement: (a) an almost immediate down-regulation of genes involved in fermentative metabolism and the GABA shunt in parallel with the activation of several 2-OGDD-encoding genes putatively involved in coupling these changes with secondary metabolism and oxygen sensing; (b) a redirection of secondary metabolism through the down-regulation of several genes of the free phenylpropanoid pathway and the diversion of propanoid synthesis toward the methyl-erythritol phosphate route located in plastids; (c) a burst in terms of phospholipid metabolism through the specific regulation of phospholipase-encoding genes and the generation of a transient increase of PCs and PEs, likely impacting downstream signaling cascades; and (d) a rapid rearrangement of hormonal responses mainly involving transcriptional down-regulation of auxin cellular intake, increased expression of ABA-synthesis genes, and rewiring of several components of the signaling and transcriptional regulation of IAA and ABA, with putative involvement of ERFs as well.

■ ASSOCIATED CONTENT

● Supporting Information

The Supporting Information is available free of charge on the ACS Publications website at DOI: [10.1021/acs.jafc.9b00036](https://doi.org/10.1021/acs.jafc.9b00036).

Table S1. Metabolites identified using GC-MS-TOF and HILIC methods (124 metabolites). Table S3. RNA-seq quantitative validation. Table S4. DEGs (B vs A log₂ fold change) encoding proteins of the glycolytic and fermentative pathways. Figure S1. PLSDA performed on the whole set of identified metabolites, including all the tested conditions in sample sets A, B, and C (PDF) Table S2. RNA-seq data of sample sets A and B (XLSX)

■ AUTHOR INFORMATION

Corresponding Author

*E-mail: pietro.tonutti@santannapisa.it.

ORCID

Pietro Tonutti: [0000-0003-1270-1317](https://orcid.org/0000-0003-1270-1317)

Funding

This work was in part supported by a project grant to B.R. from the University of Padova (SID17_01-BIRD 2017) and a project grant to P.T. from Scuola Superiore Sant'Anna.

Notes

The authors declare no competing financial interest.

■ REFERENCES

- (1) Tonutti, P. The technical evolution of CA storage protocols and the advancements in elucidating the fruit responses to low oxygen stress. *Acta Hort.* **2015**, *1079*, 53–60.
- (2) Veltman, R. H.; Verschoor, J. A.; van Dugteren, J. H. R. Dynamic control system (DCS) for apples (*Malus domestica* Borkh. cv

'Elstar'): optimal quality through storage based on product response. *Postharvest Biol. Technol.* **2003**, *27*, 79–86.

- (3) DeLong, J. M.; Prange, R. K.; Leyte, J. C.; Harrison, P. A. A New Technology That Determines Low-oxygen Thresholds in Controlled-atmosphere-stored Apples. *HortTechnology* **2004**, *14*, 262–266.

- (4) Hennecke, C.; Koepcke, D.; Dierend, W. Storage of apples in dynamic controlled atmosphere. *Erwerbs-Obstbau* **2008**, *50*, 19–29.

- (5) Zanella, A.; Cazzanelli, P.; Rossi, O. Dynamic Controlled Atmosphere (DCA) storage by the means of chlorophyll fluorescence response for firmness retention in apple. *Acta Hort.* **2008**, *796*, 77–82.

- (6) Zanella, A.; Rossi, O. Post-harvest retention of apple fruit firmness by 1-methylcyclopropene (1-MCP) treatment or dynamic CA storage with chlorophyll fluorescence (DCA-CF). *Eur. J. Hort. Sci.* **2015**, *80*, 11–17.

- (7) Brizzolara, S.; Santucci, C.; Tenori, L.; Hertog, M.; Nicolai, B.; Sturz, S.; Zanella, A.; Tonutti, P. A metabolomics approach to elucidate apple fruit responses to static and dynamic controlled atmosphere storage. *Postharvest Biol. Technol.* **2017**, *127*, 76–87.

- (8) Zanella, A.; Cazzanelli, P.; Panarese, A.; Coser, M.; Chisté, C.; Zeni, F. Fruit fluorescence response to low oxygen stress: modern storage technologies compared to 1-MCP treatment of apple. *Acta Hort.* **2005**, *682*, 1535–1542.

- (9) Gibbs, D. J.; Lee, S. C.; Md Isa, N.; Gramuglia, S.; Fukao, T.; Bassel, G. W.; Correia, C. S.; Corbineau, F.; Theodoulou, F. L.; Bailey-Serres, J.; Holdsworth, M. J. Homeostatic response to hypoxia is regulated by the N-end rule pathway in plants. *Nature* **2011**, *479*, 415.

- (10) Licausi, F.; Kosmacz, M.; Weits, D. A.; Giuntoli, B.; Giorgi, F. M.; Voeselek, L. A. C. J.; Perata, P.; van Dongen, J. T. Oxygen sensing in plants is mediated by an N-end rule pathway for protein destabilization. *Nature* **2011**, *479*, 419.

- (11) Cukrov, D.; Zermiani, M.; Brizzolara, S.; Cestaro, A.; Licausi, F.; Luchinat, C.; Santucci, C.; Tenori, L.; Van Veen, H.; Zuccolo, A.; Ruperti, B.; Tonutti, P. Extreme Hypoxic Conditions Induce Selective Molecular Responses and Metabolic Reset in Detached Apple Fruit. *Front. Plant Sci.* **2016**, *7*, 146.

- (12) Narsai, R.; Secco, D.; Schultz, M. D.; Ecker, J. R.; Lister, R.; Whelan, J. Dynamic and rapid changes in the transcriptome and epigenome during germination and in developing rice (*Oryza sativa*) coleoptiles under anoxia and re-oxygenation. *Plant J.* **2017**, *89*, 805–824.

- (13) Paradiso, A.; Caretto, S.; Leone, A.; Bove, A.; Nisi, R.; De Gara, L. ROS Production and Scavenging under Anoxia and Re-Oxygenation in Arabidopsis Cells: A Balance between Redox Signaling and Impairment. *Front. Plant Sci.* **2016**, *7*, 1803.

- (14) Trobacher, C. P.; Clark, S. M.; Bozzo, G. G.; Mullen, R. T.; DeEll, J. R.; Shelp, B. J. Catabolism of GABA in apple fruit: subcellular localization and biochemical characterization of two γ -aminobutyrate transaminases. *Postharvest Biol. Technol.* **2013**, *75*, 106–113.

- (15) Fiehn, O. Metabolite Profiling in Arabidopsis. In *Arabidopsis Protocols*; Salinas, J., Sanchez-Serrano, J. J., Eds.; Humana Press: Totowa, NJ, 2006; pp 439–447.

- (16) Martinelli, F.; Remorini, D.; Saia, S.; Massai, R.; Tonutti, P. Metabolic profiling of ripe olive fruit in response to moderate water stress. *Sci. Hort.* **2013**, *159*, 52–58.

- (17) Joung, J.-G.; Corbett, A. M.; Fellman, S. M.; Tieman, D. M.; Klee, H. J.; Giovannoni, J. J.; Fei, Z. Plant MetGenMAP: An Integrative Analysis System for Plant Systems Biology. *Plant Physiol.* **2009**, *151*, 1758.

- (18) Diab, H.; Limami, A. Reconfiguration of N Metabolism upon Hypoxia Stress and Recovery: Roles of Alanine Aminotransferase (AlaAT) and Glutamate Dehydrogenase (GDH). *Plants* **2016**, *5*, 25.

- (19) Narayan, V. S.; Nair, P. M. Metabolism, enzymology and possible roles of 4-aminobutyrate in higher plants. *Phytochemistry* **1990**, *29*, 367–375.

(20) Takayama, M.; Ezura, H. How and why does tomato accumulate a large amount of GABA in the fruit? *Front. Plant Sci.* **2015**, *6*, 612.

(21) Michaeli, S.; Fromm, H. Closing the Loop on the GABA Shunt in Plants: Are GABA metabolism and signaling entwined? *Front. Plant Sci.* **2015**, *6*, 419.

(22) Salminen, A.; Kauppinen, A.; Kaarniranta, K. 2-Oxoglutarate-dependent dioxygenases are sensors of energy metabolism, oxygen availability, and iron homeostasis: potential role in the regulation of aging process. *Cell. Mol. Life Sci.* **2015**, *72*, 3897–3914.

(23) Cheng, A.-X.; Han, X.-J.; Wu, Y.-F.; Lou, H.-X. The Function and Catalysis of 2-Oxoglutarate-Dependent Oxygenases Involved in Plant Flavonoid Biosynthesis. *Int. J. Mol. Sci.* **2014**, *15*, 1080.

(24) Hagel, J. M.; Facchini, P. J. Expanding the roles for 2-oxoglutarate-dependent oxygenases in plant metabolism. *Nat. Prod. Rep.* **2018**, *35*, 721–734.

(25) Bailey-Serres, J.; Fukao, T.; Gibbs, D. J.; Holdsworth, M. J.; Lee, S. C.; Licausi, F.; Perata, P.; Voesenek, L. A. C. J.; van Dongen, J. T. Making sense of low oxygen sensing. *Trends Plant Sci.* **2012**, *17*, 129–138.

(26) Brunetti, C.; Fini, A.; Sebastiani, F.; Gori, A.; Tattini, M. Modulation of Phytohormone Signaling: A Primary Function of Flavonoids in Plant-Environment Interactions. *Front. Plant Sci.* **2018**, *9*, 1042.

(27) Shiono, K.; Yamauchi, T.; Yamazaki, S.; Mohanty, B.; Malik, A. I.; Nagamura, Y.; Nishizawa, N. K.; Tsutsumi, N.; Colmer, T. D.; Nakazono, M. Microarray analysis of laser-microdissected tissues indicates the biosynthesis of suberin in the outer part of roots during formation of a barrier to radial oxygen loss in rice (*Oryza sativa*). *J. Exp. Bot.* **2014**, *65*, 4795–4806.

(28) Harwood, J. L. Phosphoglycerides of mitochondrial membranes. In *Methods in Enzymology*; Academic Press, 1987; Vol. 148, pp 475–485.

(29) Xie, L.-J.; Yu, L.-J.; Chen, Q.-F.; Wang, F.-Z.; Huang, L.; Xia, F.-N.; Zhu, T.-R.; Wu, J.-X.; Yin, J.; Liao, B.; Yao, N.; Shu, W.; Xiao, S. Arabidopsis acyl-CoA-binding protein ACBP3 participates in plant response to hypoxia by modulating very-long-chain fatty acid metabolism. *Plant J.* **2015**, *81*, 53–67.

(30) Mustroph, A.; Zanetti, M. E.; Jang, C. J. H.; Holtan, H. E.; Repetti, P. P.; Galbraith, D. W.; Girke, T.; Bailey-Serres, J. Profiling transcriptomes of discrete cell populations resolves altered cellular priorities during hypoxia in Arabidopsis. *Proc. Natl. Acad. Sci. U. S. A.* **2009**, *106*, 18843.